ChemComm

COMMUNICATION

View Article Online
View Journal | View Issue

Cite this: *Chem. Commun.*, 2015, **51**, 3211

Received 17th December 2014,
Accepted 12th January 2015

DOI: 10.1039/c4cc10064f

www.rsc.org/chemcomm

Synthesis of colloidal Janus nanoparticles by asymmetric capping of mesoporous silica with phenylsilsesquioxane†

Hiroto Ujiie,[a] Atsushi Shimojima*[a] and Kazuyuki Kuroda*[ab]

Colloidal mesoporous silica nanoparticles asymmetrically capped with non-porous phenylsilsesquioxane have been prepared by adding phenyltriethoxysilane to an aqueous dispersion of mesostructured silica–surfactant composite nanoparticles. The integration of colloidal stability, mesoporosity and the Janus structure is quite promising for materials design applicable in various fields, including catalysis, biomedicine and coatings.

Janus particles with asymmetric structures or surface properties have attracted great interest because these particles exhibit unusual behaviour that cannot be observed for isotropic particles.[1–3] A typical example is Janus particles with hydrophilic and hydrophobic faces, which are assembled at oil–water interfaces to form water repellent membranes[4] and Pickering emulsions.[5] The Janus-type structure is also important for maximising the functions of individual components without interfering with each other. Precise design based on the type, size and shape of each component promises a wide range of applications in displays, sensors and drug delivery systems, although the easy and large-scale fabrication of Janus particles remains a major challenge.

Mesoporous silica nanoparticles (<100 nm in diameter) possess high surface areas, large pore volumes, tunable pore sizes and modifiable surfaces, which make these particles potentially useful as catalysts,[6] drug-delivery carriers,[7,8] and coatings.[9] Recently, Janus-type mesoporous silica particles with magnetite and metal counterparts have been prepared by the anisotropic growth of mesostructured silica on the core particles[10] and by sputtering metals on a monolayer of mesoporous silica particles,[11,12] respectively. Zhao and co-workers reported the synthesis of Janus particles by the growth of mesoporous organosilica on mesoporous silica particles.[13] Nonetheless, the types of mesoporous silica-based Janus particles reported so far have been very limited and their particle sizes are generally greater than 100 nm. Further development of a synthetic approach is therefore significant from both scientific and practical points of view.

Herein, we report a new class of mesoporous Janus nanoparticles prepared by adding phenyltriethoxysilane (PTES) to a dispersion of colloidal mesostructured silica–surfactant composite nanoparticles (hereafter denoted as CMSS). The obtained Janus nanoparticles (<50 nm in diameter) possess an asymmetric structure, where a mesoporous silica nanosphere is capped with a nonporous, hemispherical phenylsilsesquioxane shell (see Fig. 1). Although post-modification of mesoporous silica nanoparticles with organosilane is a well-established method for their functionalisation,[14–17] this report is the first on asymmetric modification to produce Janus nanoparticles. In addition to the differences in the hydrophobicity, reactivity and thermal–mechanical properties of silica and phenylsilsesquioxane, the combination of porous and nonporous components will be useful for designing unique nanocarriers, nanocoatings and complex assemblies.

CMSS with an average particle diameter of 30 nm (Fig. S1 in ESI†) were prepared according to our previous report.[18] The molar composition of the starting mixture was 1 tetraethoxysilane (TEOS), 0.50 cetyltrimethylammonium bromide (CTAB), 0.25 triethanolamine (TEA), and 1200 H_2O. To the dispersion of CMSS (pH 8.2),

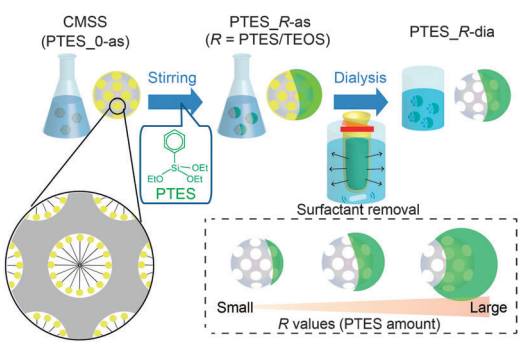

Fig. 1 Synthetic procedure for the Janus nanoparticles. The green parts represent phenylsilsesquioxane ($PhSiO_{1.5}$).

[a] *Department of Applied Chemistry, Faculty of Science and Engineering, Waseda University, 3-4-1 Ohkubo, Shinjuku-ku, Tokyo 169-8555, Japan. E-mail: shimojima@waseda.jp, kuroda@waseda.jp; Fax: +81-3-5286-3199*
[b] *Kagami Memorial Research Institute for Materials Science and Technology, Waseda University, 2-8-26 Nishiwaseda, Shinjuku-ku, Tokyo 169-0051, Japan*

† Electronic supplementary information (ESI) available: Experimental details, Table S1 and Fig. S1–S7. See DOI: 10.1039/c4cc10064f

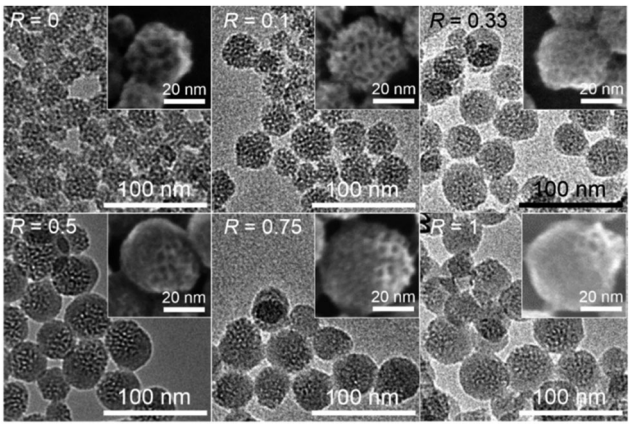

Fig. 2 TEM and FE-SEM (insets) images of PTES_*R*-dia.

PTES was added, and the mixture was stirred at 80 °C for 12 h. The dispersion was then dialysed with a mixture of 2 M acetic acid and ethanol (7 : 3 v/v) to remove the surfactant (see the ESI† for details). The samples before and after dialysis are denoted as PTES_*R*-as and PTES_*R*-dia, respectively, where *R* is the molar ratio of PTES to TEOS used for the preparation of nanoparticles.

Fig. 2 shows transmission electron microscopy (TEM) and field-emission scanning electron microscopy (FE-SEM) images of the nanoparticles prepared with varying amounts of PTES (PTES_*R*-dia). The core particles before growth ($R = 0$) have worm-like mesopores with open pores on their surfaces. When $R \geq 0.5$, it is clearly shown that the core particles are capped with a hemispherical shell with smooth surfaces.

The size of the non-porous shell increases with an increase in the amount of added PTES. An increase of the C contents was also confirmed (Fig. S2 in ESI†). When $R = 0.5$, the C/Si ratio evaluated by the CHN analysis and thermogravimetry was 2.4, which is relatively higher than that corresponding to the ratio of phenyl groups to Si atoms in the dispersion (C/Si = 2.0). The difference in the C/Si ratios is possibly because of the adsorption of cetyltrimethylammonium (denoted as C_{16}TMA) cations and/or to the higher solubility of silica compared with that of organosiloxane in an aqueous solution under near neutral to basic conditions.[19–21] As a control experiment, the reaction of PTES in an aqueous solution of CTAB and TEA without CMSS was observed to yield dispersed nanoparticles approximately 10 nm in diameter (data not shown). In the PTES_*R*-dia samples, the coexistence of these nanoparticles was not confirmed by TEM, suggesting that PTES was mostly consumed for the capping of CMSS.

The growth of hemispherical shells during the reaction was monitored by TEM (Fig. 3). At early stages of the reaction (0–5 min), asymmetric structures were not clearly observed. After 10 min, non-porous shells were clearly observed (lower right part of the particle), and the shells subsequently became thicker (~1 h). Further growth of the shell was not notably observed during 1–6 h, which indicates the completion of hydrolysis and condensation of PTES. This trend in the growth of the shell was also confirmed by CHN analysis; the C content gradually increased and became constant after 1 h (Table S1 in ESI†).

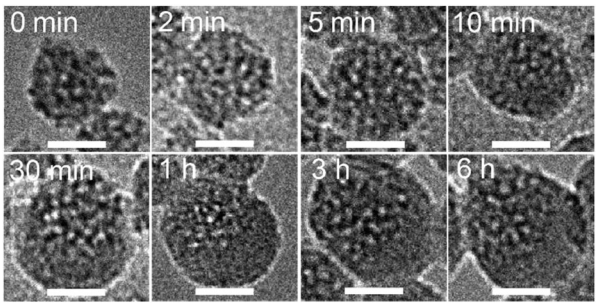

Fig. 3 Evolution of the morphology of the nanoparticles ($R = 0.5$) during the reaction observed by TEM. The time lapse after the addition of PTES to the CMSS dispersion is shown in each image. The surfactants were removed by dialysis before the observations. Scale bars: 20 nm.

The dispersions of CMSS before and after dialysis (PTES_0-as and PTES_0-dia, respectively) were almost transparent, while those of PTES_0.5-as and PTES_0.5-dia became translucent (Fig. 4A). Although the Rayleigh scattering becomes stronger after the shell formation, the dynamic light scattering (DLS) measurements of all these samples reveal single peaks at approximately 50 nm and the absence of any peaks over a few hundred nanometres, indicating good dispersibility even after the shell formation and subsequent surfactant removal (Fig. 4B). The particle diameters measured by DLS do not precisely match the real particle size observed by TEM but are at least overestimated due to the hydration layer around the particles.

The ζ potential values of PTES_0.5-as and -dia were almost the same (+51 mV and +52 mV, respectively), while those of PTES_0-as and -dia were largely different (+47 mV and +3 mV, respectively). The positive potentials can be ascribed to the C_{16}TMA cations adsorbed on the surface of the particles,[18] leading to the high dispersibility of the particles. For PTES_0.5-dia, the amount of residual C_{16}TMA ions was relatively large compared with PTES_0-dia. CHN analysis revealed that ~6% of C_{16}TMA cations remained in PTES_0.5-dia, whereas the amount of residual C_{16}TMA ions in PTES_0-dia was under the detection limit. This difference is possibly because of

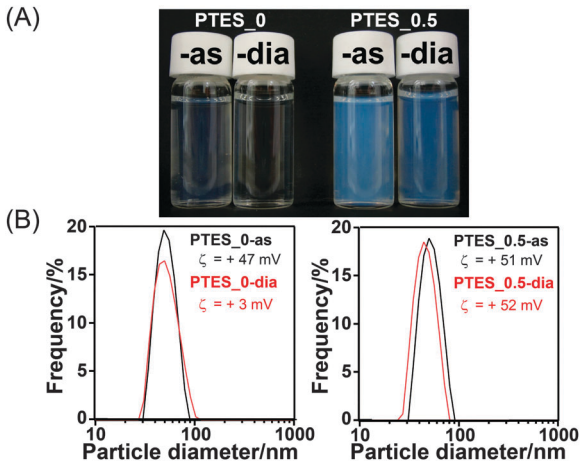

Fig. 4 (A) Appearances of PTES_0-as, PTES_0-dia, PTES_0.5-as and PTES_0.5-dia. (B) Particle diameter distributions of the nanoparticles measured by dynamic light scattering (DLS) (inset: ζ potentials of each sample).

hydrophobic interactions between the alkyl chains of C_{16}TMA ions and the phenyl groups on the nanoparticles.

The ^{29}Si CP/MAS NMR spectrum of PTES_0.5-dia (Fig. S3 in ESI†) consists of the signals assigned to T^2, T^3 (T^x represents $PhSi(OH)_{3-x}(OSi)_x$), Q^3 and Q^4 (Q^y represents $Si(OH)_{4-y}(OSi)_y$) units at −69.0 ppm, −78.1 ppm, −100.0 ppm and −110.1 ppm, respectively, confirming that phenylsilsesquioxane was formed and that the silica networks originating from the core nanoparticles were retained. In the IR spectrum of PTES_0.5-dia (Fig. S4 in ESI†), new peaks assigned to phenyl groups are clearly observed. Importantly, the degree of condensation of the Q units ($Q^4/(Q^3 + Q^4)$) is apparently higher than that before the reaction with PTES, suggesting that phenylsiloxane units are covalently attached to the surface of mesoporous silica nanoparticles by Si–O–Si bonds.

The nitrogen adsorption/desorption isotherms and pore size distributions of PTES_0-dia and PTES_0.5-dia are shown in Fig. 5. Both samples exhibit a type-IV curve, suggesting the presence of mesopores. The pore size distributions reveal two peaks corresponding to intraparticle mesopores (<5 nm) and interparticle voids (>10 nm). The Brunauer–Emmett–Teller (BET) surface area and pore volume of PTES_0.5-dia were calculated to be 430 $m^2\ g^{-1}$ and 0.75 $cm^3\ g^{-1}$, respectively. These values are smaller than those of PTES_0-dia (BET surface area: 780 $m^2\ g^{-1}$, pore volume: 1.6 $cm^3\ g^{-1}$), suggesting that the shell is essentially non-porous. The smaller pore size of PTES_0.5-dia (*ca.* 3.2 nm) compared with that of PTES_0-dia (*ca.* 4.3 nm) is not attributed to residual surfactants because a similar pore size resulted when the surfactant was almost completely removed under more severe conditions. It is plausible that the phenylsilsesquioxane units exist not only in the shell but also on the surface of the inner mesopores. When the amount of PTES was varied in the range of R = 0.1–1.0, the pore size was almost constant (*ca.* 3.0 nm), independent of the R value (Fig. S5 in ESI†). This fact indicates that a relatively small portion of PTES is involved in the surface modification of the mesopores, and the remaining portion is consumed for the growth of the shell.

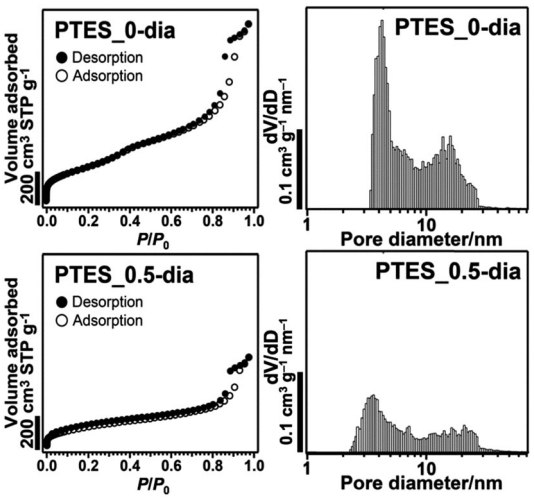

Fig. 5 (left) Nitrogen adsorption/desorption isotherms and (right) pore size distributions (calculated by the NLDFT method) of PTES_0-dia and PTES_0.5-dia.

Growth of CMSS by the addition of tetraalkoxysilane has recently been reported.[22] In this case, isotropic growth of the mesostructured shell occurs, while the pore size of the core particles is unchanged. The decrease of the pore size (~1 nm) observed for PTES_0.5-dia can be explained by the amphiphilic nature of hydrolysed PTES molecules to facilitate their penetration into the internal surfactant assemblies in CMSS. A substantial amount of free surfactants is also present in the liquid phase of the dispersion of CMSS. The formation of the non-porous phenylsilsesquioxane shell despite the presence of surfactant is consistent with the general findings that mesostructures cannot be formed from organotrialkoxysilane alone.[23]

The formation mechanism of the hemispherical shell is not clearly understood, but appears to be related to the hydrolysis rate of PTES. Generally, hydrolysis of alkoxysilane under basic conditions proceeds *via* OH^- attack against centred Si. Compared with TEOS, PTES is hydrolysed much more slowly because of the steric and inductive effects of phenyl groups.[24] In our system, therefore, the added PTES exists as an oil phase for a relatively long period. A slow supply of hydrolysed PTES to the water phase should favour the continuous growth of the particles initially formed on CMSS without additional nucleation. It is also possible that CMSS are located at the interface between water and PTES oil droplets as an emulsifier; hence, nucleation and growth essentially occur on one side of CMSS. To verify the importance of the slow hydrolysis rate, we used pre-hydrolysed PTES (Fig. S6 in ESI†). Hydrolysis of PTES under weakly acidic conditions was performed according to a previous report.[25] After the addition of the pre-hydrolysed solution to the dispersion of CMSS, a homogeneous dispersion without PTES droplets was obtained immediately. The TEM image of the resulting sample demonstrated that asymmetric structures were not formed (Fig. S7 in ESI†). A phenylsilsesquioxane shell was formed uniformly around the core nanoparticles. Similarly, the Janus structure was not observed when methyltriethoxysilane (MTES) was used instead of PTES, which can be explained by the relatively high hydrolysis rate of MTES. Thus, the proper selection of organoalkoxysilane is the key to the asymmetric shell formation.

Notably, the mesoporous silica parts in our Janus particles can be selectively etched with aq. Na_2CO_3 based on the higher solubility of silica compared with organosiloxane.[20,21] The selective silica etching of PTES_0.5-dia produced cap-like nanoparticles (Fig. 6), demonstrating the hemispherical shape of the shell. This finding is in contrast to the generation of hollow

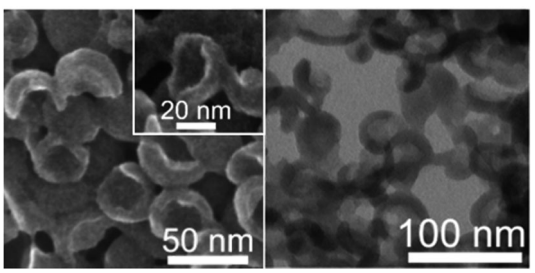

Fig. 6 FE-SEM (left) and scanning TEM (right) images of PTES_0.5-dia after selective etching of the mesoporous silica component.

nanoparticles (Fig. S7 in ESI†) by etching of the aforementioned isotropically grown particles prepared using pre-hydrolysed PTES.

In conclusion, colloidal mesoporous Janus nanoparticles have been successfully prepared by the addition of phenyltriethoxysilane to an aqueous dispersion of mesostructured silica nanoparticles. The high dispersibility, mesoporosity and structural asymmetry of the Janus nanoparticles are potentially useful, especially for applications as phase-selective catalysts or drug-delivery carriers. These nanoparticles are also attractive as building blocks to create higher order structures.

The authors thank Mr K. Onishi and E. Yamamoto (Waseda Univ.) for discussion. They also thank Mr M. Yoshikawa (Waseda Univ.) for his help on NMR measurement. This work was supported in part by a Grant-in-Aid for Challenging Exploratory Research (No. 25620191) and by a Grant-in-Aid for Scientific Research on Innovative Areas ''New Polymeric Materials Based on Element-Blocks (Area No. 2401)'' from the Ministry of Education, Culture, Sports, Science and Technology (MEXT), Japan.

Notes and references

1 J. Hu, S. Zhou, Y. Sun, X. Fang and L. Wu, *Chem. Soc. Rev.*, 2012, **41**, 4356.
2 A. Walther and A. H. E. Müller, *Chem. Rev.*, 2013, **113**, 5194.
3 G. Loget and A. Kuhn, *J. Mater. Chem.*, 2012, **22**, 15457.
4 S.-H. Kim, S. Y. Lee and S.-M. Yang, *Angew. Chem., Int. Ed.*, 2010, **49**, 2535.
5 F. Liang, K. Shen, X. Qu, C. Zhang, Q. Wang, J. Li, J. Liu and Z. Yang, *Angew. Chem., Int. Ed.*, 2011, **50**, 2379.
6 Y. Huang, S. Xu and V. S.-Y. Lin, *Angew. Chem., Int. Ed.*, 2011, **50**, 661.
7 J. L. Vivero-Escoto, I. I. Slowing, B. G. Trewyn and V. S.-Y. Lin, *Small*, 2010, **6**, 1952.
8 C. Argyo, V. Weiss, C. Bräuchle and T. Bein, *Chem. Mater.*, 2014, **26**, 435.
9 Y. Hoshikawa, H. Yabe, A. Nomura, T. Yamaki, A. Shimojima and T. Okubo, *Chem. Mater.*, 2010, **22**, 12.
10 L. Zhang, F. Zhang, W.-F. Dong, J.-F. Song, Q.-S. Huo and H.-B. Sun, *Chem. Commun.*, 2011, **47**, 1225.
11 M. Xuan, J. Shao, X. Lin, L. Dai and Q. He, *ChemPhysChem*, 2014, **15**, 2255.
12 X. Ma and S. Sanchez, *Chem. Commun.*, DOI: 10.1039/c4cc08285k.
13 X. Li, L. Zhou, Y. Wei, A. M. El-Toni, F. Zhang and D. Zhao, *J. Am. Chem. Soc.*, 2014, **136**, 15086.
14 Y.-S. Lin, N. Abadeer, K. R. Hurley and C. L. Haynes, *J. Am. Chem. Soc.*, 2011, **133**, 20444.
15 J. M. Rosenholm, A. Meinander, E. Peuhu, R. Niemi, J. E. Eriksson, C. Sahlgren and M. Lindén, *ACS Nano*, 2009, **3**, 197.
16 J. Kobler, K. Möller and T. Bein, *ACS Nano*, 2008, **2**, 791.
17 V. Cauda, A. Schlossbauer, J. Kecht, A. Zürner and T. Bein, *J. Am. Chem. Soc.*, 2009, **131**, 11361.
18 C. Urata, Y. Aoyama, A. Tonegawa, Y. Yamauchi and K. Kuroda, *Chem. Commun.*, 2009, 5094.
19 H. Yamada, C. Urata, Y. Aoyama, S. Osada, Y. Yamauchi and K. Kuroda, *Chem. Mater.*, 2012, **24**, 1462.
20 C. Urata, H. Yamada, R. Wakabayashi, Y. Aoyama, S. Hirosawa, S. Arai, S. Takeoka, Y. Yamauchi and K. Kuroda, *J. Am. Chem. Soc.*, 2011, **133**, 8102.
21 N. Koike, T. Ikuno, T. Okubo and A. Shimojima, *Chem. Commun.*, 2013, **49**, 4998.
22 E. Yamamoto, M. Kitahara, T. Tsumura and K. Kuroda, *Chem. Mater.*, 2014, **26**, 2927.
23 W. Wang, J. E. Lofgreen and G. A. Ozin, *Small*, 2010, **6**, 2634.
24 C. J. Brinker and G. W. Scherer, *Sol-Gel Science: The Physics and Chemistry of Sol-Gel Processing*, Academic Press, 1990.
25 M. Kuniyoshi, M. Takahashi, Y. Tokuda and T. Yoko, *J. Sol–Gel Sci. Technol.*, 2006, **39**, 175.

